Counterion and Temperature Effects on Aqueous Ionic Perfluoropolyether Micellar Solutions by Small-Angle Neutron Scattering

C. M. C. Gambi,*,† R. Giordano,‡ A. Chittofrati,§ R. Pieri,§ P. Baglioni,⊥ and J. Teixeira‖

Department of Physics, University of Florence and I.N.F.M., v. G. Sansone 1, 50019 Sesto Fiorentino, Firenze, Italy, Department of Physics, University of Messina and I.N.F.M., Salita Sperone 31, 98010 S.Agata, Messina, Italy, R and D Center, Colloid Laboratory, Solvay Solexis, vl. Lombardia 20, 20021 Bollate, Milano, Italy, Department of Chemistry, University of Florence and C.S.G.I., v. della Lastruccia 3, 50019 Sesto Fiorentino, Firenze, Italy, and Laboratoire Léon Brillouin, CEA-CNRS Saclay, 91191 Gif sur Yvette Cédex, France

Received: July 29, 2003

The effect of concentration and temperature on the microstructure of aqueous micelles of carboxylic perfluoropolyether surfactants, with two perfluoroisopropoxy units in the chain ($n2$) that is chlorine-terminated, are studied by SANS for the ammonium and potassium counterions. The SANS spectra have been analyzed by a two-shell model for the micellar form factor and a screened Coulombic plus steric repulsion potential for the structure factor in the frame of the mean spherical approximation of a multiion system reduced to an effective one component macroions system (OCM). At 28 °C, in the surfactant concentration range 0.05 to 0.12 M, the micelles display spherical shape with inner core radius of 15 Å for both counterions, and interfacial layer thickness of 4 Å. At higher concentration, both counterions provide ellipsoidal micelles, with axial ratio 2 and a limiting dimension of 13 Å. A sharp increase of temperature up to 80 °C enables the ammonium salt at 0.2 M to rearrange its ellipsoidal micelles into spherical ones, while the micelles of the potassium salt remain ellipsoidal. In all cases, the micellar size distribution is extremely narrow and the average aggregation numbers, as well as the surface charge, are found to slightly differ for the two counterions upon variation of concentration and temperature, driving ionization degrees globally spanning from 0.3 to 0.5. The interfacial hydration, the surface potential and the area per polar head at the micellar surface are discussed too.

Introduction

Perfluoropolyether (PFPE) carboxylic salts, belonging to the wide family of fluorinated amphiphiles, are known to form a wide range of self-association structures in water, spanning from liquid crystals[1–3] to microemulsions with fluorinated oils, either of oil-continuous types[4–6] or a water-continuous type[7] of interest in fluoropolymers manufacturing.[8–9]

Literature data are available on the structure of micelles of perfluorinated surfactants, namely perfluoroalkyl carboxylates in aqueous solution,[10–12] while no structural studies were available for the PFPE analogues, since a preliminary SANS work from our group.[13] This work examined the micellar solutions of ammonium or potassium salts of an high purity acid of the type Cl(C$_3$F$_6$O)$_2$CF$_2$COOH, having two perfluoroisopropoxy units in the tail ($n2$). The results suggest that a transition from spherical to anisotropic micelles occurs, at constant temperature, with both salts upon increasing concentration.

With the same surfactants, the present work enlarges the previous study[13] with respect to the range of concentration and temperature, providing a deeper insight in the micellization and intermicellar interaction of these laterally branched PFPE salts. The whole body of the SANS results is now presented. It confirms that spherical micelles form at relatively low concentration or high temperature, with narrow size distribution. Then, increasing the concentration or reducing the temperature the occurrence of ellipsoidal micelles is suggested.

The ammonium salt solutions of the same PFPE acid have been recently studied by time-resolved fluorescence quenching[14] and by conductivity,[15] so further details on the micellar growth and shape transition as micellar interactions are expected shortly, while a wider range of counterions and chain lengths is being presently studied by SANS.

Modeling Micelles

To study the micellar system by SANS the scattered neutron intensity was measured as a function of the scattering wave vector **Q**. The micellar solution is assumed composed by surfactant molecules at the critical micellar concentration, cmc, and micelles with an average surfactant aggregation number N and an effective micellar charge Q^*.

To define the normalized particle form factor $P(Q)$, the micelle has been modeled as a two-shell particle, formed of a core containing the surfactant chlorine-terminated perfluoropolyether tails and an interfacial layer containing the surfactant polar headgroups CO$_2^-$, some counterions X$^+$, and hydration water molecules. The net separation between the fluorinated and the hydrogenated region of the micelle is hypothesized on the basis of high hydrophobicity of fluorinated molecules.[16] For the particle form factor $P(Q)$ we use two different models that will be detailed below. In one case the shape of the micelles is spherical, in the other ellipsoidal.

† University of Florence and I.N.F.M.
‡ University of Messina and I.N.F.M.
§ Solvay Solexis.
⊥ University of Florence and C.S.G.I.
‖ CEA-CNRS Saclay.
* Corresponding author.

SANS of PFPE Aqueous Micellar Solutions

J. Phys. Chem. A, Vol. 107, No. 51, 2003 **11559**

The interparticle structure factor $S(Q)$ is the result of steric repulsion and screened Coulombic repulsion between micelles[17-19] and it has been calculated assuming an analytical solution for the multicomponent ionic liquid with a mean spherical approximation (MMSA).[20-22] The multicomponent system was reduced to an effective one-component macroions (OCM) system[19,23] under Gillan's condition.[24] A detailed description of the theoretical framework is reported in refs 25 and 26. According to theory, the total neutron cross section per unit volume of the sample can be written as[27]

$$I(Q) = C_M N (\sum_i b_i - V_m \rho_s)^2 P(Q) S(Q) + I_{back}$$

where C_M is the number density of the surfactant molecules in micelles ($C_M = C - cmc$, with C being the surfactant concentration and cmc the critical micellar concentration), N is the average surfactant aggregation number of the micelle already defined, Σb_i is the total scattering length of all the atoms in the surfactant molecule, V_m is the surfactant molecule volume, or monomer volume, and ρ_s is the scattering density of the solvent, i.e., the H_2O scattering length divided by the H_2O molecule volume. I_{back} is the spectrum background. The term $\Sigma_i b_i - V_m \rho_s$ represents the contrast, i.e., the difference between the scattering length of the dry surfactant molecule and the solvent molecules of equivalent volume. We can define the scattering length density of the two parts of a micelle. ρ_1 is the scattering length density of the hydrophobic core, which is equal to the total scattering length of the surfactant tail divided by the tail volume, V_{tail}. ρ_2 is the scattering length density of the shell, which is given by the sum of the scattering lengths of the atoms in the shell divided by the shell volume V_{shell} and can be written as follows:

$$\rho_2 = \frac{N}{V_{shell}} [N_S b_{H_2O} + b_{CO_2^-} + (1-\alpha) b_{X^+}]$$

where $\alpha = Q^*/N$ is the fractional ionization and represents the number of free X^+ counterions surrounding each micelle (this number corresponds to the number of unscreened surfactant heads of a micelle), $(1-\alpha)$ is the number of X^+ ions per surfactant molecule in the micellar shell and N_S is the hydration number per surfactant molecule defined by:[25]

$$N_S = \left[\frac{V_{shell}}{N} - (V_m - V_{tail})(1-\alpha) - (V_m - V_{tail} - V_{X^+})\alpha \right] \frac{1}{V_{H_2O}}$$

with V_{X^+} being the volume of the dry counterion.

In the spectral analysis, the scattering length density of the micellar core ρ_1 must be introduced as known parameter. Thus, first of all the volume of the surfactant molecule was obtained from the MW of the surfactant and from the surfactant density extrapolated from the density measurements of several aqueous surfactant solutions with the ammonium surfactant. Once found the volume of the surfactant molecule, the volume of the tail was obtained by subtracting the volume of the counterion[28] and of the polar head (CO_2^-, $V = 35.3$ Å^3 estimated by the universal force field method[29]). The values of the MW, volume, scattering length, and scattering length density for the different parts of the micellar solution are reported in Table 1. The chlorine atom is a portion of the surfactant tail that can be either in the tail end termination or in a branched configuration of the final part of the molecule. The contrast between the chlorine atom and

TABLE 1: Molecular Weight (MW), Volume (V), Scattering Length (sl) and Scattering Length Density (ρ) of the Cl(C₃F₆O)₂CF₂ Tail Group, Polar Head, Counterions, Solvent, and Chlorine Atom

	MW	V (Å^3)	sl (10^{-12} cm)	ρ (10^{10} cm^{-2})
tail	417	384	14.68	3.823
CO_2^-	44	35.26	1.826	5.179
NH_4^+	18	13.58	-0.566	-4.168
K^+	39	11.01	0.367	3.338
H_2O	18	29.9	-0.1677	-0.5609
Cl	35.5	39	0.957	2.456

the other part of the tail is small, thus it was neglected. The main contrast is between the surfactant tail (with chlorine atom included) and the interfacial layer. Another contrast is between the interfacial layer and the solvent.

For the particle structure factor $P(Q)$ we used two different models.

(a) Spheres. The micelles are considered spheres in the solution. The form factor $P(Q)$ therefore is

$$P(Q) = \int_0^\infty |F(Q, R)|^2 f(R) \, dR$$

where $f(R) \, dR$ is the normalized density of probability of a sphere having a total radius (core plus shell) between R and $R + dR$.[30] The distribution that describes better the polydispersity in the micellar solution is the Schulz distribution.[30] Within the two-shell micellar model, if R is the total radius of the micelle and pR is the core radius (where p is a parameter with values $0 < p < 1$), the form factor of single particle can be written[31]

$$F(Q, R) = p^3 (\rho_1 - \rho_2) V_{total} F_0(QpR) + (\rho_2 - \rho_s) V_{total} F_0(QR)$$

where:

$$F_0(x) = \frac{3 j_1(x)}{x}$$

with j_1 being the first-order Bessel function. Assuming a Schulz distribution, the overall micellar form factor $P(Q)$ is reported in detail in ref 31 and was recently summarized in ref 32.

The coherent scattered intensity for a system of polydispersed interacting micelles is

$$I(Q) = C_M N (\sum_i b_i - V_m \rho_s)^2 P(Q)[1 + \beta(Q)(S(Q) - 1)] + I_{back}$$

where

$$\beta(Q) = \frac{|\langle F(Q) \rangle|^2}{P(Q)}$$

The average radius of the particle core R_c, the polydispersity of size, N, Q^*, and the shell thickness t are free fitting parameters.

(b) Ellipsoids. The micelle is a two-shell ellipsoidal aggregate composed by an inner region, the hydrophobic core, made up of the close-packed surfactant tails, with principal axes a, b, b, and the hydrophilic layer, with a thickness t, composed of headgroups (CO_2^-), a fraction of counterions (NH_4^+ or K^+) and hydration water molecules.[33-34] A priori, a can be larger or smaller than b leading to prolate or oblate ellipsoids, respectively. In this model, $P(Q)$ is given by[34]

$$P(Q) = \int_0^1 |F(Q,\mu)|^2 \, d\mu$$

where $F(Q,\mu)$ is the form factor of the two-shell single particle and $\mu = \cos \vartheta$ with ϑ angle between the direction of the **Q** vector and the symmetry axis, a, of the ellipsoid. The integral represents the average over all the possible orientations of the particle. Because of the two-shell model

$$F(Q,\mu) = f\frac{3j_1(u)}{u} + (1-f)\frac{3j_1(v)}{v}$$

with

$$u = Q[\mu^2 a^2 + (1-\mu^2)b^2]^{1/2}$$

$$v = Q[\mu^2(a+t)^2 + (1-\mu^2)(b+t)^2]^{1/2}$$

and

$$f = \frac{V_T(\rho_1 - \rho_2)}{\left(\sum_i b_i - V_m\rho_s\right)}$$

$j_1(u)$ and $j_1(v)$ are the first-order Bessel functions of argument u and v respectively. We have to notice that N, Q^*, b, and t are independent parameters. a is obtained as

$$a = \frac{NV_{tail}}{\frac{4}{3}\pi b^2}$$

thus it depends on the free parameters N and b.

The diameter of the equivalent spherical micelle is $D = 2((a + t)(b + t)^2)^{1/3}$. The total volume of the micelle $V_{total} = (4/3)\pi (a + t)(b + t)^2$ leads to the calculation of the shell volume $V_{shell} = V_{total} - NV_{tail}$.

(c) Interaction Potential. In both models the macroion–macroion (or micelle–micelle) interaction effective potential[17-19,23] is

$$\frac{U(x)}{K_BT} = U_1\frac{\exp(-k(x-1))}{x}$$

for $x > 1$, where $x = r/D$; r is the distance from the center of the micelle, D is the micelle diameter, $k = k_D D$ is the screen constant where k_D is the inverse of the Debye length, l_D. The latter is related to the surfactant concentration and cmc, to temperature and to the free parameters Q^* and N.

U_1 is the contact potential, i.e., the potential on the micellar surface ($r = D$):

$$U_1 = \frac{(Q^*e)^2}{4\pi K_BTD\epsilon\left(1 + \frac{k}{2}\right)^2}$$

where e is the electronic charge, $\epsilon = \epsilon_0\epsilon_r$ is the product of dielectric constant of vacuum ϵ_0 and the dielectric constant of solvent. The macroion structure factor was calculated using a revised version of Hayter–Penfold's Fortran package.[17]

The parameter η represents the volume fraction of micelles:

$$\eta = \frac{(C - cmc)N_A}{N}\frac{4\pi}{3}(R_c + t)^3$$

where N_A is the Avogadro number and R_c represents the average core radius for spherical micelles or the equivalent spherical core radius for ellipsoidal micelles.

Materials

The samples of ammonium and potassium salts of the carboxylic acid $Cl(C_3F_6O)_2CF_2COOH$ have been provided by Solvay Solexis (formerly Ausimont), with purity of 99.8% with respect to the formula, yet including two isomers due to the terminal group. The molecular weight of the acid, by titration and NMR, agreed within 5% experimental error with the calculated value of 462. The salts, prepared with ammonia or potassium hydroxide of RPE grade in Milli-Q-grade water, were free of acid and inorganic impurities within analytical sensitivities. Milli-Q water has been used for all the solutions of this work.

The micellization and phase behavior in water of the same ammonium salt used here and also the sodium salt of the same acidic precursor have been previously detailed.[7,14-15] The threshold concentration for liquid crystal formation at 25 °C in water is around 25 wt % for the ammonium salt, well above the concentrations of the present work. The potassium salt is expected to have even higher concentration threshold, as detectable by optical microscopy in polarized light. Caboi et al.,[1-2] using a mixture of homologous PFPE carboxylates with average MW slightly higher than the present sample, had shown by NMR the liquid crystalline phase in equilibrium with the micellar solution to be of lamellar type (L_α) for either ammonium or potassium salt solutions, with threshold concentration much higher in the case of the potassium salt, namely 12.5 wt % against the 7 wt % for the ammonium salt.

The ammonium salt, indicated by n2NH$_4$, has critical micellar concentration, at 25 °C, of 2.1×10^{-2} M as obtained by equilibrium surface tension[7] with accuracy of 8% on four different samples from the same purification procedure. The cmc value was substantially confirmed by conductivity along with evidence of Krafft temperature below 15 °C.[15] The cmc of the potassium salt, n2K, 1.8×10^{-2} M at 25 °C has been measured here in the same conditions previously used[7] by Du Nouy method, with a Lauda TE1C tensiometer connected to a thermostatic bath and applying to raw force data the Harkins–Jordan correction factors. Each equilibrium value at a fixed concentration was obtained by 5–6 measurements, with experimental deviation decreasing from 0.2 mN/m in the lowest concentration range to 0.05 mN/m in the plateau of the surface tension–concentration curve. A negligible variation of cmc for ammonium and sodium salt solutions had been assessed up to 40 °C,[7] so the values obtained at 25 °C are used at a temperature of 28 °C, selected here for n2 salts in analogy with work in progress with longer-chain analogues more prone to solubility constraints. At 80 °C, the cmc value is 1.3×10^{-2} M for the n2NH$_4$ and 1.1×10^{-2} for the n2K potassium salt.

The density of the aqueous solutions of the ammonium salt has been measured as a function of concentration by a PAAR DMA 5000 density meter at 28 ± 0.1 °C thus obtaining the density of the ammonium salt, 1.836 g/cm^3.

Two series of samples were studied by SANS for each salt, to study the concentration and the temperature dependence.

Method

SANS experiments were performed at the spectrometer PAXE (Lab. Léon Brillouin, Saclay, France) with a sample–detector distance of 2.55 m and incident neutron wavelength of 5 Å with wavelength spread of 10%. Collimation was achieved by two slits of 12 and 7 mm placed 2.5 m far apart. Samples were
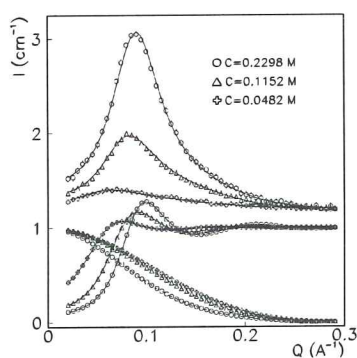
Figure 1. Experimental scattered intensity vs Q of micellar solutions with ammonium counterion at temperature of 28 °C and concentrations of 0.2298 (circles), 0.1152 (triangles), and 0.0482 M (crosses). The continuous lines on the data points are the fitted curves. The corresponding normalized form and structure factors are reported in the bottom of the figure for each sample (identical symbols of the data points) connected by dashed and continuous lines, respectively. The vertical scale of the normalized form and structure factors is dimensionless.
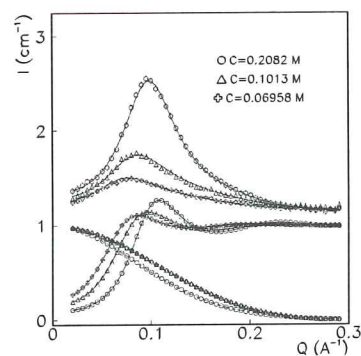

Figure 2. Experimental scattered intensity vs Q of micellar solutions with potassium counterion at temperature of 28 °C and concentrations of 0.2082 (circles), 0.1013 (triangles), and 0.06958 M (crosses). The continuous lines on the data points are the fitted curves. The corresponding normalized form and structure factors are reported in the bottom of the figure for each sample (identical symbols of the data points) connected by dashed and continuous lines, respectively. The vertical scale of the normalized form and structure factors is dimensionless.

contained in flat quartz cells of thickness 1 mm, and measured at 28, 40, and 80 °C with a thermal stability of ±0.1 °C. The two-dimensional intensity distributions were corrected for the background and the empty cell contributions and then normalized to absolute intensity by dividing them with a scattering intensity of a secondary standard of known cross-section.[25,35] By integrating the normalized two-dimensional intensity distribution with respect to the azimuthal angle, one-dimensional scattering intensity distributions $I(Q)$ in the unit of a differential cross section per unit volume (cm^{-1}) were obtained.

We have to point out that the favorable contrast of the samples makes possible the neutron scattering measurements without isotopic substitution. On the contrary, the light scattering investigation is very hard because of the poor contrast between the water phase and the fluorinated phase (index of refraction 1.33 and 1.28, respectively).

Results

The experimental spectra at 28 °C are represented in Figure 1 for ionic micellar solutions with ammonium counterion at surfactant concentration C of 0.2298, 0.1152, and 0.0482 M, and in Figure 2 with potassium counterion at concentration C of 0.2082, 0.1013, and 0.06958 M. $I(Q)$, the scattered neutron cross section per unit volume of the sample, is reported vs the momentum transfer Q. The spectra are characterized by a sharp structural peak which is a manifestation of strong interactions between the micelles. A decrease of concentration for both the ammonium and potassium surfactants leads to a strong decrease of the peak intensity and to a shift of the peak position. In Figures 3 and 4, the experimental spectra are reported for the samples with C = 0.2180 M (ammonium counterion) at 28, 40, and 80 °C, and with $C = 0.2116$ M (potassium counterion) at 28 and 80 °C.

The fitting procedure of the experimental data to the theoretical models above-reported has been performed for all the samples in the explored thermal range. In Figure 5 is reported an example of experimental spectrum and fitted curve with the extracted form and structure factor for one sample. In Figures 1−4, the fitted curves (continuous lines) and the form and structure factors (dashed and continuous lines, respectively) are reported for each sample. In the concentration range 0.05 to 0.1 M at T = 28 °C the model which fits the experimental
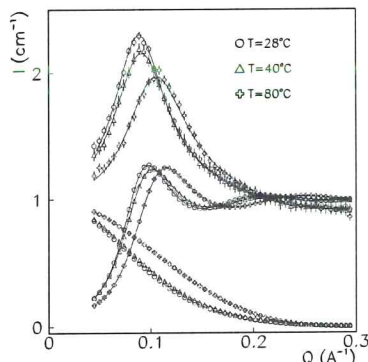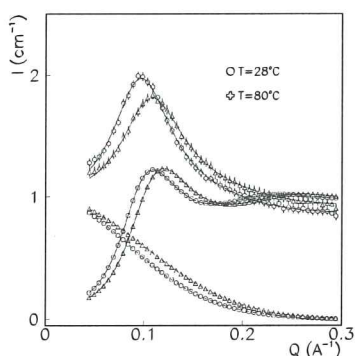

Figure 3. Experimental scattered intensity vs Q of micellar solutions with ammonium counterion with concentration of 0.2180 M at three temperature values of 28 (circles), 40 (triangles) and 80 °C (crosses). The continuous lines on the data points are the fitted curves. The corresponding normalized form and structure factors are reported in the bottom of the figure for each sample (identical symbols of the data points) connected by dashed and continuous lines, respectively. The vertical scale of the normalized form and structure factors is dimensionless.

spectra is the sphere model for both counterions. The fitting parameters $Q*$, N, t, R_c are evaluated for the samples studied and are reported in Table 2. The polydispersity of the micellar size was also evaluated leading to values of 10% that we consider due to the intrinsic polydispersity of the measurements. At a concentration of 0.2 M, only the ellipsoidal model fits the data for both counterions. The fitting parameters $Q*$, N, b, and t are evaluated for the samples studied and are reported in Table 2. b and R_c are reported in the same column; when the a/b axial ratio is given, the value of the column is b, when the axial ratio is not given, the micelles are spherical and the value of the column is R_c. D represents twice the average core radius for spherical micelles or twice the equivalent spherical core radius for the ellipsoidal ones.

The quality of the fit was deduced by the reduced χ^2 value, which is always very close to 1 as shown in Table 2.

The numerical results for all the samples studied are reported in Table 2 where in addition to the free fitting parameters values, the other parameters useful to characterize the micellar solutions and deduced as detailed in a previous paragraph are also reported, i.e., the micelle diameter D, the ellipsoidal axial ratio

Figure 4. Experimental scattered intensity vs Q of micellar solutions with potassium counterion with concentration of 0.2116 M at two temperature values of 28 (circles) and 80 °C (triangles). The continuous lines on the data points are the fitted curves. The corresponding normalized form and structure factors are reported in the bottom of the figure for each sample (identical symbols of the data points) connected by dashed and continuous lines, respectively. The vertical scale of the normalized form and structure factors is dimensionless.
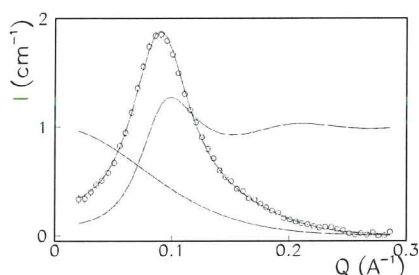
Figure 5. Experimental scattered intensity (circles), fitted curve, form and structure factors (continuous lines) for the sample of Figure 1 with $C = 0.2298$ M. Only the coherent part of the experimental spectrum is shown (the solvent spectrum has been subtracted). The vertical scale is dimensionless for the normalized form and structure factors.

a/b, the number of interfacial water molecules for surfactant molecule N_S, the Debye length l_D, the contact potential U_1, and the volume fraction of micelles in solution η.

Discussion

From the reported SANS results, at a temperature of 28 °C, it is clearly shown that aggregates are found in solution with microstructural properties typical of ionic micelles in solution. At low surfactant concentration, in the range 0.05 to 0.1 M, the ammonium and potassium micelles are spherical. As the concentration is increased above 0.2 M, the shape becomes that of a prolate ellipsoid for both micellar solutions. The increase of temperature from 28 up to 80 °C leads the ammonium ellipsoidal micelles to become spherical, whereas for the potassium micelles the ellipsoidal shape is maintained.

The micellar inner core is defined by the average core radius R_c for the spherical micelles and by the short and long axis b and a, respectively, for the ellipsoidal micelles. The R_c and b values represent the fluorinated tail length in the micelle, 13–15 Å for ammonium and 12–14 Å for potassium micelles, thus very similar. The interfacial layer thickness, t, is 3.8 Å for the ammonium micelles and 4.1 Å for the potassium micelles. Thus, in the concentration range investigated, the fluorinated chain length of the surfactant molecule defines the micellar inner core size and the carboxylic head defines the micellar interfacial thickness. Temperature does not significantly affect these geometrical results. Furthermore, it is possible to evaluate the area per polar head of the micellar inner and outer surface by

R_c and t values for the spherical micelle and by a, b, and t values for the ellipsoidal micelles. These values are reported in Table 3. Values in the ranges 70–80 and 115–130 Å^2 for inner and outer surfaces, respcetively, have been found for ammonium micelles as well as values of 70–95 (inner) and 120–170 Å^2 (outer) for potassium micelles.

For both counterions, the average diameter of the micelles decreases weakly vs both the concentration decrease and the temperature increase.

At 28 °C, the net micellar surface charge depends weakly on the counterion and changes slightly vs concentration for both counterions. The average aggregation number is 57 and less than 40 for ammonium counterion at high and low surfactant concentration respectively, whereas it is ~40 and ~30 for potassium (same trend vs concentration). The latter parameter depends strongly on the counterion as also found for hydrogenated micelles.[21]

The ionization degree, $\alpha = Q^*/N$, spans from 0.33 to 0.48 for ammonium micelles and from 0.41 to 0.45 for potassium micelles. The surfactant carboxylic polar heads are surrounded by almost 10 water molecules for ammonium and 13 water molecules for potassium micelles. The increase of temperature produces a decrease of N for both counterions and an increase of α that are independent of the shape change.

Debye's length and contact potential increase vs the concentration decrease whereas the increase of temperature does not affect significantly Debye's length and decreases the contact potential.

An important characteristic of the OCM model is that the size of the micelles must be irrelevant for long-range interactions between micelles. In fact, the micelle is modeled as a point charge.[19,23] Thus, the micelles concentration rather than the micelle diameter dominates the structure and the appropriate length scale for correlations between micelles is the point charge radius defined as $R_{pc} = D/(2\eta^{1/3})$. Taking into account the η dependence on the surfactant concentration above-reported, $R_{pc} \sim ((C - cmc)/N)^{-1/3}$. This dependence can be verified by plotting the Q_{max} (value of Q corresponding to the peak position of the structure factor) vs $((C - cmc)/N)^{-1/3}$. In Figures 6 and 7, this dependence is reported for ammonium and potassium micelles, respectively, calculating the abscissa from surfactant concentration values, cmc values of both micellar solutions and N as obtained by the fits (Table 2). The trend is linear as expected.

In summary, ionic chlorine terminated perfluoropolyether micelles have been studied by SANS with a two-shell model for the micellar form factor and a screened Coulombic plus steric repulsion potential for the structure factor in the frame of the mean spherical approximation of a multiion system reduced to an effective one component macroions system (OCM). The latter represents the charged micelles, surrounded by an ionic cloud of some counterions located in the region defined by Debye's length, dispersed in the continuous medium. The microstructure of the micellar solutions of this work is well-defined in the concentration range 0.05–0.23 M and from 28 up to 80 °C. The micelles are monodispersed spheres at low surfactant concentration and monodispersed ellipsoids at high concentration, at 28 °C. The increase of temperature for the ellipsoidal micelles leads to spherical micelles only for the ammonium counterion. The diameter of the micelles is ~40 Å. The radius of the inner core is 15 Å for the spherical micelles and 13 (short axis) and ~30 Å (long axis) for the ellipsoidal micelles. The interfacial thickness is 4 Å. Thus, the microstructure is very similar for both counterions. The aggregation number and the

TABLE 2: SANS Results of PFPE Ionic Micellar Solutions with Ammonium (NH$_4^+$) and Potassium (K$^+$) Counterions at Temperatures of 28, 40 and 80 °C^a
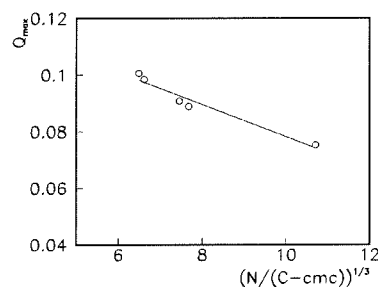
C (M)	Q^*	N	t (Å)	$R_c(b)$ (Å)	α	D (Å)	a/b	N_S	l_D (Å)	U_1 (K_BT)	η	χ^2
						NH$_4^+$						
						28 °C						
0.2298	19	57	3.7	13	0.33	42	2.2	9.0	13	8.5	0.089	1.1
0.1152	17	39	4.0	15	0.44	39		11	15	10	0.044	1.1
0.0482	16	33.5	3.8	15	0.48	37		11	18	13	0.013	1.0
						28 °C						
0.2180	19	57	3.8	13	0.33	43	2.4	10	13	8.8	0.085	1.1
0.1095	15	40	4.0	15	0.38	39		12	16	8.2	0.041	1.1
						40 °C						
0.2180	17	52	3.8	12	0.33	42	2.5	11	15	7.5	0.091	1.0
						80 °C						
0.2180	15	36	3.8	15	0.42	37		11	14	6.7	0.095	1.2
						K$^+$						
						28 °C						
0.2082	16.6	40.3	4.1	12	0.41	39	2.0	12	13	7.7	0.091	1.1
0.1013	14	31	4.1	14	0.45	36		13	16	8.1	0.041	1.0
0.069 58	14	31	4.0	14	0.45	36		13	17	9.7	0.025	1.0
						28 °C						
0.2116	14	42	4.1	12	0.33	40	2.0	12	13	5.9	0.093	1.2
0.1067	13	34	4.0	14	0.38	37		12	16	7.2	0.042	1.1
						80 °C						
0.2116	13	31	4.0	12	0.42	37	1.9	13	14	5.6	0.100	1.0

^{a} C is the molar surfactant concentration. Q^* is the effective charge, N the average aggregation number, t the micellar shell thickness, R_c the micellar core radius, b the micellar inner minor axis, α the fractional ionization, D the diameter of the equivalent spherical micelle, a/b the axial ratio with a major axis of the micelle, N_s the hydration number, l_D Debye's length, U_1 the potential on the micellar surface, η the volume fraction of the micelles, and reduced χ^2.

TABLE 3: Inner and Outer Surface per Polar Head Calculated by the Results of Table 2

C (M)	Σ_{inner} (Å^2)	Σ_{outer} (Å^2)
	NH$_4^+$	
	28 °C	
0.2298	69	114
0.2180	75	125
0.1152	73	116
0.1095	71	113
0.0482	84	133
	40 °C	
0.2180	72	126
	80 °C	
0.2180	79	123
	K$^+$	
	28 °C	
0.2116	74	133
0.2082	77	138
0.1067	72	120
0.1013	80	133
0.069 58	80	131
	80 °C	
0.2116	96	170

Figure 6. Dependence of Q_{max} as a function of the inverse of volume fraction of micelles to $^1/_3$, for ammonium micelles at 28 °C.
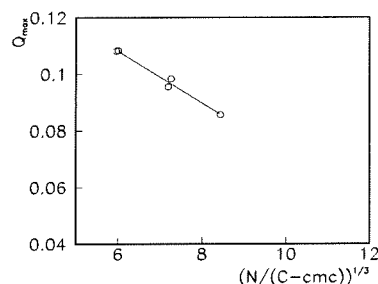
Figure 7. Dependence of Q_{max} as a function of the inverse of volume fraction of micelles to $^1/_3$, for potassium micelles at 28 °C.

surface micellar charge are different for ammonium and potassium and lead to different ionization degrees which increase as a function of both a concentration increase or a temperature increase. The number of interfacial water molecules, the Debye length, and the contact potential are also known in details as the area per polar head at the micellar surface. Furthermore, the polar head is surrounded by 10 water molecules for the ammonium micelles and by 13 water molecules for the potassium ones. The Debye length of average value 15 Å increases weakly vs the concentration increase and does not change significantly as a function of the temperature. The contact potential depends on the counterion and decreases vs the concentration decrease as well as vs the temperature increase.

References and Notes

(1) Caboi, F.; Chittofrati, A.; Monduzzi, M.; Morioni, C. *Langmuir* **1996**, *12*, 6022−6027.

(2) Caboi, F.; Chittofrati, A.; Lazzari, P.; Monduzzi, M. *Colloids Surf. A: Physicochem. Eng. Aspects* **1999**, *160*, 47.

(3) Wurtz, J.; Meyer, J.; Hoffmann, H. *Phys. Chem. Chem. Phys.* **2001**, *3* (15), 3132.

(4) Baglioni, P.; Gambi, C. M. C.; Giordano, R.; Senatra, D. *J. Mol. Struct.* **1996**, *383*, 165−169.

(5) Baglioni, P.; Gambi, C. M. C.; Giordano, R. *Physica B* **1997**, 295−296.

(6) Monduzzi, M.; Knacksted, M. A.; Ninham, B. W. *J. Phys. Chem.* **1995**, *99*, 17772.

(7) Chittofrati, A.; D'Aprile, F.; Pieri, R.; Lenti, D.; Maccone, P.; Visca, M. Prog. Colloid Interface Sci. (proceedings of communication at XV ECIS 2001, Coimbra), in press.

(8) Giannetti, E.; Visca, M. (Ausimont, S.p. A.), U.S. Pat. 4,864,006, 1988.

(9) Giannetti, E.; Chittofrati, A.; Sanguineti, A. Proceedings of Int. Symposium on Fluorine Chemistry, Roma, May 1996. *Chim. Ind. (Milan)* **1997**, *79*, 611.

(10) Burkitt, S. J.; Ottewill, R. H.; Hayter, J. B.; Ingram, B. T. *Colloid Polym. Sci.* **1987**, *265*, 619.

(11) Berr, S. S.; Jones, R. R. M. *J. Phys. Chem.* **1989**, *93*, 2555.

(12) Iijima, H.; Kato, T.; Yoshida, H.; Imai, M. *J. Phys. Chem. B* **1998**, *102*, 990.

(13) Gambi, C. M. C.; Giordano, R.; Chittofrati, A.; Pieri, R.; Baglioni, P.; Teixeira, J. *Appl. Phys. A: Mater. Sci. Process.* **2002**, *74* [Suppl.], 5436.

(14) Sulak, K.; Szajdzinska-Pietek, E. *Proceedings of the Conference "Surfactants and Dispersed Systems in Theory and Practice", Soruz, Polanica Zdroj, May 20−23*; Wilk, K. A., Ed.; Oficyna Wydawnicza Politechniki Wrocławskiej: Wrocław, Poland, 2003.

(15) Kallay, N.; Tomii, V.; Hrust, V.; Pieri, R.; Chittofrati, A. Special issue devoted to ELKIN, Krakow, Poland. *Colloids Surf.* **2002**.

(16) Kissa, E. In *Fluorinated Surfactants*; 1994; Surfactant Science Series 50; Marcel Dekker: New York, 1994.

(17) Hayter, J. B.; Penfold, J. J. *J. Mol. Phys.* **1981**, *42* (1), 109.

(18) Hayter, J. B.; Penfold, J. J. *J. Chem. Soc., Faraday Trans.* **1981**, *77*, 1851.

(19) Snook, I. K.; Hayter, J. B. *Langmuir* **1992**, *8*, 2880−2884.

(20) Hansen, J. P.; Hayter, J. B. *Mol. Phys.* **1982**, *46*, 651−656.

(21) Sheu, E. Y.; Wu, C. F.; Chen, S.-H.; Blum, L. *Phys. Rev. A* **1985**, *32*, 3807.

(22) Senatore, G. In *Structure and Dynamics of Strongly Interacting Colloids and Supramolecular Aggregates in Solutions*; Chen, S.-H., Huang, J. S., Tartaglia, P., Eds.; Kluwer Academic Publisher: Dordrecht, The Netherlands, 1992; pp 175−189.

(23) Hunter, R. J. In *Foundation of Colloid Science*; Oxford Science Publications, Clarendon Press: Oxford, England; Oxford University Press: New York, 1989; Vol. 2, Chapter 14.

(24) Gillan, M. J. *Phys. C* **1974**, *7*, L1−L4.

(25) Liu, Y. C.; Baglioni, P.; Teixeira, J.; Chen, S.-H. *J. Phys. Chem.* **1994**, *98*, 10208.

(26) Liu, Y. C.; Ku, C. K.; Lo Nostro, P.; Chen, S.-H. *Phys. Rev. E* **1995**, *51*, 4598.

(27) Sheu, E. Y.; Chen, S.-H.; Huang, J. S. *J. Phys. Chem.* **1987**, *91*, 1535.

(28) Yizhak, Marcus. In *Ion Properties*; Marcel Dekker: New York, 1997; p 46.

(29) Rappe, A. K.; Casewit, C. J.; Colwell, K. S.; Goddard, W. A., III; Skiff, W. M. *J. Am. Chem. Soc.* **1992**, *114*, 10024 with additional parameters (for dummy atoms) from: Castonguay, L. A.; Rappe, A. K. *J. Am. Chem. Soc.* **1992**, *114*, 5832. Rappe, A. K.; Colwell, K. S. *Inorg. Chem.* **1993**, *32*, 3438.

(30) Kotlarchyk, M.; Chen, S.-H. *J. Chem. Phys.* **1983**, *79*, 2461.

(31) Hayter, J. B. In *Physics of Amphiphiles: Micelles, Vescicles and Microemulsions*; Degiorgio, V., Corti, M., Eds.; North-Holland: Amsterdam (Elsevier Science: New York), 1985; p 59.

(32) Scaffei, L.; Lanzi, L.; Gambi, C. M. C.; Giordano, R.; Baglioni, P.; Teixeira, J. *J. Phys. Chem.* **2002**, *106*, 10771−10776.

(33) Chao, Y. S.; Sheu, E. Y.; Chen, S.-H. *J. Phys. Chem.* **1985**, *89*, 4862.

(34) Chen, S.-H. *Annu. Rev. Phys. Chem.* **1986**, *37*, 351.

(35) Teixeira, J. In *Structure and Dynamics of Strongly Interacting Colloids and Supramolecular Aggregates in Solutions*; Chen, S.-H., Huang, J. S., Tartaglia, P., Eds.; Kluwer Academic Publisher: Dordrecht, The Netherlands, 1992; pp 635−658.